Mechatronics 21 (2011) 166–175

Contents lists available at ScienceDirect

Mechatronics

journal homepage: www.elsevier.com/locate/mechatronics

Holistic system modeling in mechatronics

Robin Chhabra, M. Reza Emami *

Institute for Aerospace Studies, University of Toronto, 4925 Dufferin Street, Toronto, Ontario, Canada M3H 5T6

ARTICLE INFO

Article history:
Received 10 March 2010
Accepted 6 October 2010
Available online 18 November 2010

Keywords:
Bond graphs
Concurrent design
Holistic design criteria
Mechatronic system modeling
Mechatronics
Multidisciplinary system design

ABSTRACT

This paper outlines an alternative modeling scheme for mechatronic systems, as a basis for their concurrent design. The approach divides a mechatronic system into three generic subsystems, namely *generalized executive, sensory* and *control*, and links them together utilizing a combination of bond graphs and block diagrams. It considers the underlying principles of a multidisciplinary system, and studies the flow of energy and information throughout its different constituents. The first and second laws of thermodynamics are reformulated for mechatronic systems, and as a result three holistic design criteria, namely *energy, entropy* and *agility*, are defined. These criteria are formulated using the bond graph representation of a mechatronic system. As a case study, the three criteria are employed separately for concurrent design of a five degree-of-freedom industrial robot manipulator.

1. Introduction

Mechatronics is a synergistic approach to the design, development and manufacturing of multidisciplinary engineering systems, where the emphasis is on the physical integration and information communication amongst various subsystems in a holistic fashion [1]. The synergy must be rooted into how such systems are viewed as a unified physical entity, instead of a collection of several subsystems. Consequently, the criteria based on which mechatronic systems are designed and evaluated must refer to universal characteristics, in addition to specific performance indexes. In the traditional design approaches different modeling schemes are employed for the subsystems separately, and a collection of objectives are defined to be optimized given the constraints that are enforced by each individual subsystem. These approaches often undermine the interconnection between the subsystems, which can play a significant role in the overall performance of a multidisciplinary system. The necessity of collaboration and information communication amongst the subsystems of a mechatronic system highlights the importance of a holistic approach to its modeling, which is capable of viewing all the subsystems with different physical domains from a unified perspective.

In this paper a generic interpretation of mechatronic systems is introduced based on the notion of information and energy flow throughout the system. Accordingly, a combination of bond graphs and block diagrams is used to represent mechatronic systems. The analogy between mechatronic and thermodynamic systems is formalized, and the laws of thermodynamics are reformulated for defining some global design criteria that deem the system as a whole.

Several attempts have been launched to unify the dynamic equations of mechatronic systems that consist of strongly-coupled mechanical, electrical, and control components. For instance, linear graph theory has been utilized for modeling various physical systems since the mid 1960s. It was originally employed in modeling of electrical networks [2], but gradually extended to multibody systems [3], and eventually mechatronic systems [4]. This approach tries to graphically connect the topological representation of a system to the physical characteristics of engineering components. The intention is to reduce the complexity of the governing equations in a formal way. Physical variables, namely *through* (e.g. force or current) and *across* (e.g. displacement or voltage), on each edge are defined based on their methods of measurement [5]. The *terminal* relations between the variables and the system topology are used to extract a system of mixed differential and algebraic equations in a matrix form [6].

Alternatively, in the early 60s the concept of energy and energy exchange was realized as a common notion to all components of a system with different physical disciplines [7]. Later, the concept of port in electrical circuits was generalized to power port, labeled as *power bond*, in an arbitrary physical domain [8]. The resulting modeling scheme, called *bond graphs*, is a domain-independent graphical description of dynamical behaviour of multidisciplinary systems. Similar to the graph theoretic approach, it emphasizes that the analogy between different domains is more than the pure mathematical equations, and the actual physical concepts are analogous. Therefore, in bond graphs components of a system are recognized by the energy they supply or absorb, store or dissipate, and

* Corresponding author. Tel.: +1 416 946 3357; fax: +1 416 946 7109.
E-mail addresses: chhabrar@utias.utoronto.ca (R. Chhabra), emami@utias.utoronto.ca (M. Reza Emami).

0957-4158/$ - see front matter © 2010 Elsevier Ltd. All rights reserved.
doi:10.1016/j.mechatronics.2010.10.003

reversibly or irreversibly transform [9]. This technique was extended to complex mechanical systems in three-dimensional space by introducing *multibond* (*vector bond*) *graphs* [10,11], and it has recently been applied for modeling and design of mechatronic systems [12–15]. In [16,17], mechatronic systems have been modeled by bond graphs, and the multi-objective design problem is solved using genetic algorithms. In this paper bond graphs are utilized to introduce an energy-based method of modeling for a generic subsystem of any mechatronic system, called generalized executive subsystem. This method is helpful to the synergy of the model in two ways: (a) by unifying the definition of system constituents in various physical domains, and (b) by considering the interconnections between different subsystems in the form of energy transmission. As a result, the system can be deemed as a whole in a design process.

The following section gives a quick review of the bond graphs that are extensively used in the coming sections. In Section 3, mechatronic systems are formally defined, and a suitable modeling scheme for their concurrent design is suggested. In Section 4, the first and second laws of thermodynamics are formulated for a mechatronic system using bond graph notations. Section 5 defines three holistic design criteria, namely *energy, entropy* and *agility*, based on the laws of thermodynamics for mechatronics. Section 6 presents a case study, where the developed criteria are used separately for the concurrent synthesis of a five degree-of-freedom (d.o.f.) industrial robot manipulator, and the three different designs are compared. Some concluding remarks are made in Section 7.

2. Bond graph modeling: an overview

A bond graph model represents the entire dynamics of a system by considering the power exchange between its different components or subsystems. This method unifies the system components modeling by categorizing the system variables, such as velocity, force, current and voltage into two major groups called *flow* and *effort*. These two generalized variables can be multiplied at each instant to identify the amount of power transmitted between the components of the system. The resulting simulation scheme, at the computational level, uses the dynamic equations of the system components and initial and boundary conditions to determine the system variables according to the principle of conservation of energy. The mathematical model deduced through this technique is equivalent to the complete dynamic model of the system, including non-linear terms. For example, for the mechanical subsystem of the manipulator studied in Section 6, this model is a graphical representation of the recursive Newton–Euler equations of motion [15].

2.1. Basic elements

Bond graphs are graphical representation of a system as a combination of its components (or subsystems) and their relationship in terms of power transactions. The system constituents are shown by letters, and the transaction of power between each pair is shown by a directed line, indicating the *reference direction* of the power flow. (A half-arrow is used for the direction of power flow to distinguish it from a signal flow in a block diagram representation.) The directed lines are called (*power*) *bonds*. Each power bond connects two system constituents through their gates, called (*power*) *ports*. Each component or subsystem can have multiple ports. Fig. 1 illustrates a basic bond graph. The amount of power (P) transmitted at each instant (t) can be determined by the product of two power variables (or power conjugates), namely *flow* (f) and *effort* (e) [15]. *Flow* and *effort* can be scalars or vectors,

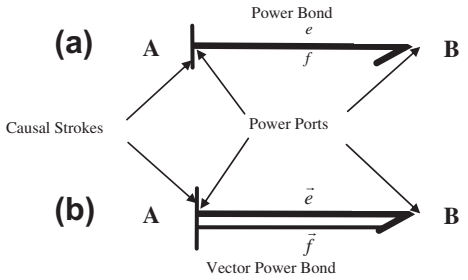

Fig. 1. (a) Power bond and, (b) vector power bond connecting power ports of elements A and B.

depending on the system constituents. In case of vectors, the bond is shown by a double-line (half) arrow, and the power is the scalar product of *flow* and *effort* vectors:

$$P(t) = \vec{e}(t) \cdot \vec{f}(t). \tag{1}$$

Table 1 lists the analogies used for *effort* and *flow* in various physical domains [9]. Although power conjugates can be different physical entities in different domains, their product always represents the power as a scalar quantity. In a bond graph system model, physical components are mapped onto conceptual elements that can capture their full dynamic behaviour [8]. These elements are divided into three main categories: (a) single-port, (b) double-port and (c) multi-port elements.

2.1.1. Single-port elements

Single-port elements consist of three generic types: *source* (*sink*) elements (S), *storage* elements (I, C), and dissipative elements (R) [12]. The S element is an ideal source (sink) of either *flow* (S_f) or *effort* (S_e). This element contains a power port, and the bond is either coming out of the element (for a source) or going toward it (for a sink). The *flow* or *effort* that a source (sink) provides (drains) can vary in time. In this case, the source (sink) is identified by MS_f or MS_e, standing for *modulated source* (*sink*). A modulated source (sink) has an additional port, called *signal port*, to identify the amount of *flow* or *effort* at each time.

Storage elements accumulate energy and release it back into the system. Depending on whether $\vec{p} \equiv \int \vec{e}(t)dt$ (*generalized momentum*) or $\vec{q} \equiv \int \vec{f}(t)dt$ (*generalized displacement*) is conserved, storage elements are divided into two categories: C and I. In type C, e.g., a capacitor or spring, the *generalized displacement* is conserved, whereas in type I, e.g., an inductor or mass, the *generalized* momentum is conserved. Both types of storage elements transform the energy reversibly. The irreversible transformation of energy that is pumped to the environment, as heat, noise, etc., is often modeled as loss or waste of energy, shown by a *dissipative* (R) element. Table 1 presents the element analogies in various energy domains. The corresponding constitutive equations of I, C, and R elements, respectively, are:

$$\vec{e}_I(t) = \widehat{I}\frac{d\vec{f}_I(t)}{dt}, \tag{2a}$$

$$\vec{f}_C(t) = \widehat{C}\frac{d\vec{e}_C(t)}{dt}, \tag{2b}$$

$$\vec{e}_R(t) = \widehat{R}\vec{f}_R; \tag{2c}$$

where $\widehat{I}$ and $\widehat{C}$ are the resistance of the I and C elements against the change of *flow* and *effort*, respectively, and $\widehat{R}$ is the resistance of the R element against the *flow* transmission.

Table 1
Bond graph elements in various energy domains.

Energy domain	*Effort* (*e*)	*Flow* (*f*)	Generalized momentum (*p*)	Generalized displacement (*q*)	*C*	*I*	*R*
Translational mechanics	Force	Velocity	Momentum	Displacement	Spring	Inertia	Damper
Rotational mechanics	Torque	Angular velocity	Angular momentum	Angle	Rotational spring	Moment of inertia	Rotational damper
Electronics	Voltage	Current	Linkage flux	Charge	Capacitor	Inductor	Resistance
Magnetics	Magnetomotive Force	Magnetic flux rate	–	Magnetic flux	Magnetic capacitor	–	Reluctance
Hydraulics	Total pressure	Volume flow rate	Pressure momentum	Volume	Reservoir	Fluid inertia	Flow resistance
Thermodynamics	Temperature	Entropy flow rate	–	Entropy	Heat capacitor	–	Heat resistance
Chemical	Chemical potential	Molar flow	–	Molar mass	–	–	–

2.1.2. Double-port elements

It can be shown that independent of energy domains only two types of ideal double-port elements can exist [8]. The first type is *transformer* (TF), which relates *effort* at one port to *effort* at the other port by a (matrix) parameter called *transformer ratio* (*N*),

$$\vec{e}_1(t) = N\vec{e}_2(t) \overset{\text{energy conservation}}{\rightarrow} \vec{f}_2(t) = N\vec{f}_1(t). \tag{3}$$

If *N* is a function of time, the element should have a signal port in addition to the power ports. This kind of transformer is called *modulated transformer* and represented by *MTF*. Transformers are utilized either in the same energy domain, e.g., gearboxes and pulleys, or between different domains, such as electromotors and winches.

The second type is *gyrator* (*GY*), which relates the *flow* at one port to the *effort* at the other port by a (matrix) parameter called *gyrator ratio* (*H*),

$$\vec{e}_1(t) = H\vec{f}_2(t) \overset{\text{energy conservation}}{\rightarrow} \vec{e}_2(t) = H\vec{f}_1(t). \tag{4}$$

A gyrator is called *modulated gyrator* (*MGY*) when *H* is variable in time. Gyrators are mostly transducers representing domain transformation such as DC-motors, pumps and turbines.

2.1.3. Multi-port elements

In order to disseminate power between the subsystems distributing elements are required. These elements are denoted as *junctions* [9]. For a physical system, interchanging ports must have no influence on the constitutive equations of junctions. The *port symmetry* and power continuity properties result in two kinds of junctions, called 0- (*zero*) and 1- (*one*) *junctions* [15]. In 0-*junction* the amount of *effort* remains constant in all ports. Thus, the power continuity equation turns into:

$$\begin{aligned} &\vec{e}_1(t) = \vec{e}_2(t) = \ldots = \vec{e}_n(t), \\ &\vec{f}_1(t) + \vec{f}_2(t) + \ldots + \vec{f}_n(t) = 0; \end{aligned} \tag{5}$$

where *n* is the number of ports. An example of 0-*junction* is parallel connection in electrical circuits.

On the other hand, 1-*junction* maintains *flow* the same at all ports. Series connection in electrical circuits is an example of 1-*junction*. Considering power continuity in an 1-*junction*, the constraint equation can be derived as:

$$\begin{aligned} &\vec{f}_1(t) = \vec{f}_2(t) = \ldots = \vec{f}_n(t), \\ &\vec{e}_1(t) + \vec{e}_2(t) + \ldots + \vec{e}_n(t) = 0. \end{aligned} \tag{6}$$

2.2. Causality

In the bond graph representation, for each element, either of power conjugates can be considered as incoming or outgoing signals. However, at the computational level one of the power variables must be chosen as the input and the other one as the output of a port. The output signal is computed based on the constitutive equations. The decision of assigning causality is denoted by the *causal stroke* in the bond graph notation. *Causal stroke* is a perpendicular line at one end of the power bond that indicates the direction of the *effort* signal as whether it comes toward or goes from the element. The resultant graph is called *causal bond graphs* that can be interpreted as block diagrams with bi-directional signal flows between different pairs of its elements. However, causality assignment to each element cannot be completely arbitrary. Depending on the element's constitutive equation, the element ports can impose constraints on the connected bonds. There are four different constraints that should be treated in the causality analysis of the bond graphs [9].

2.2.1. Fixed causality

Fixed causality occurs when the equations only allow one of the power variables to be the outgoing or incoming signal. For instance, for flow sources (sinks) the output (input) is the known flow signal.

2.2.2. Constrained causality

At TF (or MTF), GY (or MGY), 0-junction, and 1-junction there exist equations between power variables of different ports. Therefore, the causality of a particular port imposes the causality of the other ports. In a transformer element one of the ports has effort-out causality, and the other port should have effort-in causality. On the other hand, at a gyrator element both ports have either effort-out or effort-in causality. At a 0-junction element, where all the efforts are the same, one port must bring in the effort and all other ports must bring in the flow. At a 1-junction element one port should bring in the flow and the rest should bring in the effort.

2.2.3. Preferred causality

At the storage elements, the causality indicates whether the integration or differentiation of the input signal should be operated, with respect to time, to calculate the output signal. The integration is always preferred because of less computational errors.

2.2.4. Indifferent causality

For all other bond graph elements, e.g., an *R* element, no constraint can be considered in assigning the causality. Hence, the direction of the input–output signals can be assigned arbitrarily, unless other elements impose a preferred direction.

3. Mechatronic system modeling

A mechatronic system is a complex combination of several subsystems. Generally, the subsystems can be divided into three categories, namely: *Generalized Executive*, *Sensory* and *Control*. Flow of energy or information links these three generic subsystems to each other [18]. Fig. 2 shows the graphical representation of mechatronic subsystems.

The generalized executive subsystem is the integration between actuator elements and executive mechanisms. The inputs of the actuators are various forms of energy, and the outputs are various types of motion that match with the attached mechanisms. The mechanisms receive the corresponding motion, and create another form of motion. Depending on the type of the actuators, the flow of various sorts of energy can be traced throughout a generalized executive subsystem. Although in the generalized executive subsystem there exist several types of elements and subsystems from different physical domains, the universal concept of power and power exchange is common to all of them. Consequently, an energy-based model can deem all the subsystems together with their interconnections, and introduce generic criteria suitable for mechatronic system design. As it was discussed in Section 2, bond graphs are able to offer such a universal model of mechatronic systems.

A sensory subsystem consists of sensors and signal processing units that perceive *flow* or *effort* in a bond graph model, and process them to send out the required feedback signals for controlling *flow* or *effort* of the generalized executive subsystem, such as velocity, force and temperature. It also attempts to make the system aware of its surrounding by measuring the environmental properties. The measured state parameters are transmitted to the control subsystem to generate control signals. Therefore, the input to the sensory subsystem is typically in the form of energy, and the output is the signals that carry the amount of power variables.

The control subsystem is composed of microprocessors (microcontrollers) and drivers. The information sent by sensory subsystem is received and processed based on the utilized control laws. The processed information flows to the driver, where this information is translated to the amount of energy that should be provided to the actuators of the generalized executive subsystem by the energy sources. Therefore, the input to this subsystem is a set of measured power variables and the output is the energy that is required for controlling *flow* or *effort* of the generalized executive subsystem.

This subsystem also plays a significant role in mechatronics. The drivers can be represented by simple *MTF* elements in bond graphs, which receive the control signal from the controller, and distribute the supplied energy accordingly. In the computational stage, bond graphs are converted into block diagrams that are commonly used to simulate control systems [15]. Hence, a block diagram representation of a control subsystem can be merged with the bond graph model of the generalized executive subsystem. However, to complete the loop and attach a control subsystem to bond graphs, transition elements, i.e. elements of sensory subsystem, are required. The ideal sensors, which are used in the proposed modeling scheme, can be simply represented by signal flows going out of the bond graphs. They carry the value of *effort* or *flow*, and enter the block diagrams. Therefore, the combination of bond graphs and block diagrams as two powerful tools of simulation will result in an alternative modeling scheme for mechatronic systems in the concurrent design process. Details of creating such a model are illustrated in Section 6, where a five d.o.f. robot is simulated.

4. Thermodynamics of mechatronic systems

From a thermodynamic perspective, a mechatronic system can be considered as a *control mass* that can exchange energy with its environment. This control mass together with the environment form an isolated system (Fig. 3). The first law of thermodynamics, which is another expression of the universal physical law of the conservation of energy, can be restated in terms of bond graph notions as: "the increase in the *energy* of a system (E) is equal to the change of *input energy* provided to the system (E_{in}) by a supplier and through the source elements, minus the change of the *effective work* done by the system on its surrounding (W) at the sink elements and minus the change of heat dissipation (Q_{irr}) of the dissipative elements." In differential form this law can be formulated as:

$$dE = dE_{in} - dW - dQ_{irr}. \tag{7}$$

The Effective work is any useful type of energy that is exchanged between a mechatronic system and its environment.

The energy of the system can be in a form of either *introversive* or *extroversive*.

Definition 1. Introversive system energy: For a mechatronic system, introversive energy (iE) is the sum of all types of energy, including internal *dynamic* or *potential* energy, stored in the storage elements of a system due to the interconnection of the system elements.

Definition 2. Introversive dynamic energy: For a mechatronic system, introversive dynamic energy (idE) is the total energy stored in the I storage elements that conserve the generalized momentum.

Definition 3. Introversive potential energy: For a mechatronic system, introversive potential energy (ipE) is the total energy stored in the C storage elements that conserve the generalized displacement.

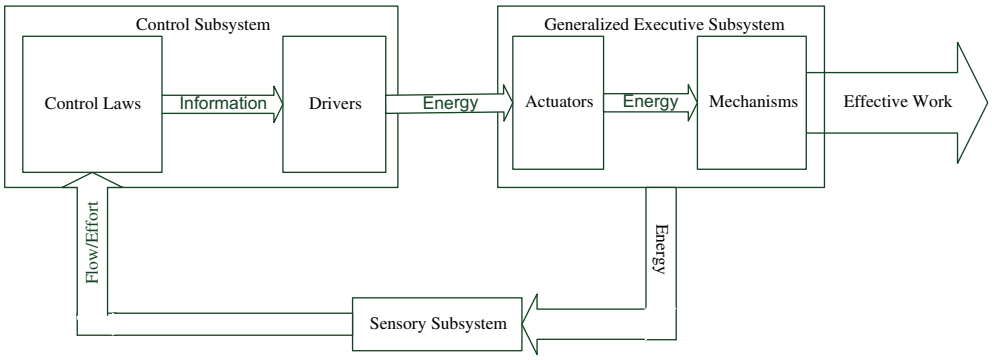

Fig. 2. Graphical representation of generic mechatronic subsystems.

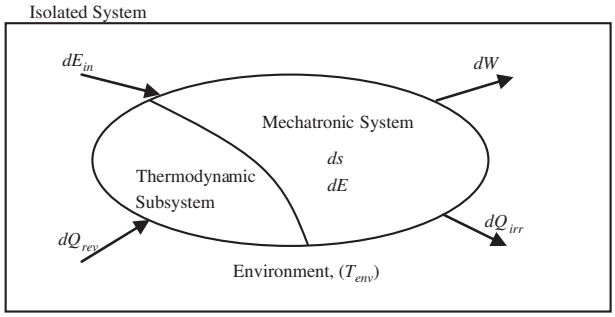

Fig. 3. Energy representation of a mechatronic system.

Based on the above definitions:

$$d(iE) = d(idE) + d(ipE). \tag{8}$$

Definition 4. Extroversive system energy: For a mechatronic system, extroversive energy (eE) is the sum of all forms of energy that are transacted between the environment and the system *as a whole* because of the physical constraints or external fields. This transaction is shown in the bond graph model of the system through source or sink elements, in addition to E_{in} and W.

Based on the above definitions, (7) can be rewritten as:

$$d(idE) + d(ipE) + dQ_{irr} = dE_{in} - d(eE) - dW, \tag{9}$$

where the change of energy state of the system elements on the left hand side is calculated from the total energy transaction between the system and environment at the sink and source elements on the right hand side of the equation.

Furthermore, the second law of thermodynamics that is basically the universal law of increasing entropy can be restated as: "the total entropy of an isolated system, i.e. the mechatronic system and its environment, which is not at equilibrium, tends to increase, and it approaches its maximum value at equilibrium." Therefore,

$$ds_{gen} = ds + ds_{env} \geqslant 0, \tag{10}$$

where s and s_{env} are the entropy of system and environment, respectively, and s_{gen} is the entropy generation of the isolated system. One can view the environment surrounding a mechatronic system as an infinite heat reservoir, isolated from the outside world, with temperature T_{env} that is assumed to be equal to the temperature of the boundary of the system.

The input energy to the system can be divided into heat (Q_{rev}), as the only form of energy that can alter the entropy, and the remaining other forms of input energy (E'_{in}):

$$dE_{in} = dE'_{in} + dQ_{rev}. \tag{11}$$

Accordingly, for every mechatronic system one can define a subsystem, namely thermodynamic subsystem, which merely exchanges heat and can be considered separately from the other parts of the system. The heat exchange process is assumed reversible, and any irreversibility effect can be modeled by a thermal dissipative element. Based on the definition of entropy in thermodynamics,

$$ds = \frac{dQ_{rev}}{T_{env}}. \tag{12}$$

In the same manner, the entropy change of the environment can be represented as:

$$ds_{env} = -\frac{dQ}{T_{env}}, \tag{13}$$

where dQ is the total heat transferred to the system; hence,

$$ds_{gen} = \frac{dQ_{rev}}{T_{env}} - \frac{dQ}{T_{env}} = \frac{dQ_{irr}}{T_{env}} \geqslant 0. \tag{14}$$

Subsequently, by substituting (7) in (14),

$$dW \leqslant d(T_{env}s - E + E'_{in}) \equiv dW_{\max}, \tag{15}$$

which implies that the change of effective work of the system is less than a maximum value ($dW_{\max}$) during the transient phase of the system, and it reaches its maximum at equilibrium when $ds_{gen} = 0$. Therefore, the *work loss* of the system, W_{loss}, can be defined as:

$$dW_{loss} \equiv dW_{\max} - dW = ds_{gen}T_{env}. \tag{16}$$

Equilibrium occurs once the entropy generation reaches its maximum value, which according to (14) is equivalent to $dQ_{irr} = 0$.

5. Holistic design criteria

This section attempts to define a number of criteria that signify the performance of a mechatronic system independently of individual subsystems, and based on the laws of thermodynamics using a bond graph system representation.

5.1. Energy criterion

Any mechatronic system is designed to perform a certain amount of effective work on its environment using the supplied input energy. Based on (9) the input energy (E_{in}) does not completely convert into the effective work (W), since portions of this energy are either stored (iE) or dissipated (Q_{irr}) in the system by its components or transacted with the environment through physical constraints or external fields (eE). The *cost energy*, defined as the sum of the energy of the system and the dissipated energy, $cE \equiv E + Q_{irr}$, is the overhead energy for performing an effective work using the supplies. The lower the cost energy, the higher the efficiency of system is. Therefore, as a design criterion $cE(W(t);t, X)$ should be minimized with respect to the design variables, X, for a desired total effective work within a time span of $[0, t_f]$ ($w_r = \int_0^{t_f} \dot{W}(t)dt$). From the first law of thermodynamics,

$$cE(t, X) = E_{in}(t, X) - W(E_{in}; t, X). \tag{17}$$

Therefore, the best design (X^*) in the set of design availabilities (A) can be achieved by

$$cE(t_f; X^*) = \min_{X \in A} cE(t_f; X). \tag{18}$$

In the bond graph system model the supplied energy is the input energy that is provided to the system at the source elements. As explained in Section 2, source elements are divided into *flow* (S_f) and *effort* (S_e). The supplied power at the ith source element (S_i), $\dot{E}_{in,i}$ is

$$\dot{E}_{in,i}(t, X) = \vec{e}_{S,i}(t; X) \cdot \vec{f}_{S,i}(t; X); \tag{19}$$

where $\vec{e}_{S,i}$ and $\vec{f}_{S,i}$ are the *effort* and *flow* in S_i, respectively. The cost energy for the period of $[0, t_f]$ can be calculated as:

$$\begin{aligned} cE(t_f; X) &= \sum_{i=1}^{N_e} \int_0^{t_f} \dot{E}_{in,i}(t; X)dt + \sum_{i=1}^{N_f} \int_0^{t_f} \dot{E}_{in,i}(t; X)dt - w_r \\ &= \sum_{i=1}^{N_e} \vec{e}_{S,i} \cdot \int_0^{t_f} \vec{f}_{S,i}(t; X)dt + \sum_{i=1}^{N_f} \vec{f}_{S,i} \cdot \int_0^{t_f} \vec{e}_{S,i}(t; X)dt - w_r \\ &= \sum_{i=1}^{N_e} \vec{e}_{S,i} \cdot \vec{q}_{S,i}(t_f; X) + \sum_{i=1}^{N_f} \vec{f}_{S,i} \cdot \vec{p}_{s,i}(t_f; X) - w_r; \end{aligned} \tag{20a-c}$$

where N_e and N_f are the number of *effort* and *flow* source elements, respectively, and $\vec{q}_{S,i}$ and $\vec{p}_{S,i}$ are the generalized displacement and momentum of S_i, respectively.

5.2. Entropy criterion

Based on the second law of thermodynamics, after a change in supplied energy, a mechatronic system reaches its equilibrium state once s_{gen} approaches its maximum. Eq. (16) shows that while reaching the equilibrium state the system capacity for doing work reduces continuously. Thus, the less the work loss, the higher the system aptitude is to perform effective work on the environment. Therefore, as an alternative design criterion $W_{loss}(E_{in}(t); X)$ should be minimized with respect to X. Referring to (16), this is equivalent to minimizing $s_{gen}(t; X)$ or $Q_{irr}(t; X)$, and accordingly it is called *entropy criterion*. Given a unit step change of supplied energy, the equilibrium time, denoted by $t_{eq}(X)$, is the time instant after which the rate of change of heat dissipation remains below a small threshold, ε,

$$t_{eq}(X) = Inf\{t_0 : \forall t > t_0 \dot{Q}_{irr}(t, X) < \varepsilon\}. \tag{21}$$

Consequently, the best design is attained in the set of design availabilities by

$$Q_{irr}(t_{eq}(X^*); X^*) = \min_{X \in A} Q_{irr}(t_{eq}(X); X). \tag{22}$$

In bond graphs the power wasted in the ith dissipative element (R_i), $\dot{Q}_{irr,i}(t; X)$, is calculated as:

$$\dot{Q}_{irr,i}(t, X) = \vec{e}_{R,i}(t; X).\vec{f}_{R,i}(t; X); \tag{23}$$

where $\vec{e}_{R,i}$ and $\vec{f}_{R,i}$ are *effort* and *flow* in R_i, respectively. Subsequently, the total heat dissipation is

$$\begin{aligned} Q_{irr}(t_{eq}(X); X) &= \sum_{i=1}^{N_R} \int_0^{t_{eq}(X)} \dot{Q}_{irr,i}(t; X) dt \\ &= \sum_{i=1}^{N_R} \widehat{R}_i \int_0^{t_{eq}(X)} \|\vec{e}_{R,i}(t; X)\|^2 dt; \end{aligned} \tag{24}$$

where N_R is the number of dissipative elements, $\| \bullet \|$ denotes the norm of a vector, and $\widehat{R}_i$ is the resistance of R_i in its constitutive equation.

5.3. Agility criterion

For systems whose response time is a crucial factor the rate of energy transmission through the system, or *agility*, can be a proper measure of design. Thus, the design criterion can be defined such that after a unit step change of some or all input parameters the time that the system needs to reach a steady state is minimized. A system reaches the steady state when the rate of its internal dynamic energy, $\dot{id}E$, becomes zero.

In the bond graph notation, idE is the total energy that is stored in I elements, and its time derivative is calculated as:

$$\begin{aligned} \dot{id}E(t; X) &= \sum_{i=1}^{N_I} \vec{e}_{I,i}(t; X).\vec{f}_{I,i}(t; X) \\ &= \sum_{i=1}^{N_I} \frac{1}{\widehat{I}_i} \vec{e}_{I,i}(t; X). \int_0^t \vec{e}_{I,i}(\tau; X) d\tau = \sum_{i=1}^{N_I} \frac{1}{\widehat{I}_i} \vec{e}_{I,i}(t; X) \vec{p}_{I,i}(t; X); \end{aligned} \tag{25a, b}$$

where N_I is the total number of I elements and $\vec{p}_{I,i}$ and $\widehat{I}_i$ are the generalized momentum and the resistance against the *flow* change of I_i, respectively.

Therefore, given a unit step change of input parameters, the response time, denoted by $T(X)$, is the time instant after which the rate of change of idE remains below a small threshold, δ,

$$T(X) = Inf\{t_0 : \forall t > t_0 \dot{id}E(t, X) < \delta\}. \tag{26}$$

As a design criterion, when the response time reaches its minimum value with respect to the design variables in the set of design availabilities the best design is attained:

$$T(X^*) = \min_{X \in A} T(X). \tag{27}$$

6. Case study

In this section kinematic, dynamic and control parameters of an industrial five d.o.f. serial-link manipulator, CRS CataLyst-5, are concurrently re-designed based on the three criteria proposed in the previous section. The kinematic characteristics are defined based on the standard Denavit–Hartenberg (D–H) convention [19]. Length (l_i), offset (d_i) and twist (α_i) of the ith link are deemed as the kinematic design variables. Each link is modeled as an L-shaped circular cylinder along link length and offset, with the cylinder radius (r_i). Thus, assuming a constant density for the ith link, r_i, l_i and d_i can be utilized to calculate the link dynamic parameters, i.e., mass, moment of inertia and location of the centre of mass. Fig. 4 depicts the robot manipulator and the link coordinate frames and definition of their D–H parameters. A servo controller (PI) with velocity feedback and feedforward is modeled to control the displacement of each manipulator joint. The control design parameters for the ith joint include proportional (P_i), integral (Int_i), velocity feedback ($Kv_{fb,i}$) and velocity feedforward ($Kv_{ff,i}$) gains. Therefore, the design problem deals with eight design parameters for each link, i.e., three D–H parameters, link cross-section radius and four control gains, and consequently, 40 variables in total.

The design problem is defined as: find the best values for the above-mentioned design variables, from their design availabilities, such that the design criterion, i.e., energy, entropy, or agility, becomes minimum, given the constraint that the end-effector (*EE*) *overall position error* determined for a set of desired trajectories remains lower than a certain amount. The average of the *EE* position error over the set of desired trajectories is a time-varying function, $E_{av}(t)$.

$$E_{av}(t) = \frac{1}{N} \sum_{i=1}^{N} \sqrt{(x_i(t) - x_{d,i}(t))^2 + (y_i(t) - y_{d,i}(t))^2 + (z_i(t) - z_{d,i}(t))^2}; \tag{28}$$

where $(x_{d,i}(t), y_{d,i}(t), z_{d,i}(t))$ are the coordinates of a point of the ith desired trajectory at the time instant t, $(x_i(t), y_i(t), z_i(t))$ are the coordinates of the *EE* point following the ith desired trajectory at the same time. The number of desired trajectories is N.

The time average of $E_{av}(t)$ can be considered as the *EE* overall position error, denoted by E_{tot}, and it is formulated as:

$$E_{tot} = \frac{1}{t_f} \sum_{i=1}^{n_t} E_{av}(t_i)(t_i - t_{i-1}); \tag{29}$$

where $\{t_i | i = 0, \ldots, n_t, t_0 = 0, t_{n_t} = t_f\}$ is a sequence of instants in which the desired trajectories are given. The initial configuration for the design problem is that of the existing industrial manipulator.

A bond graph model of a generic serial-link n d.o.f. robot manipulator including joint modules and controllers is illustrated in Fig. 5. In this figure, the *flows* and *efforts* are distinguished based on their location at the corresponding power bond. The symbol on the right-hand-side (at the bottom) of a vertical (horizontal) power bond is *effort* and the one on the left-hand-side (at the

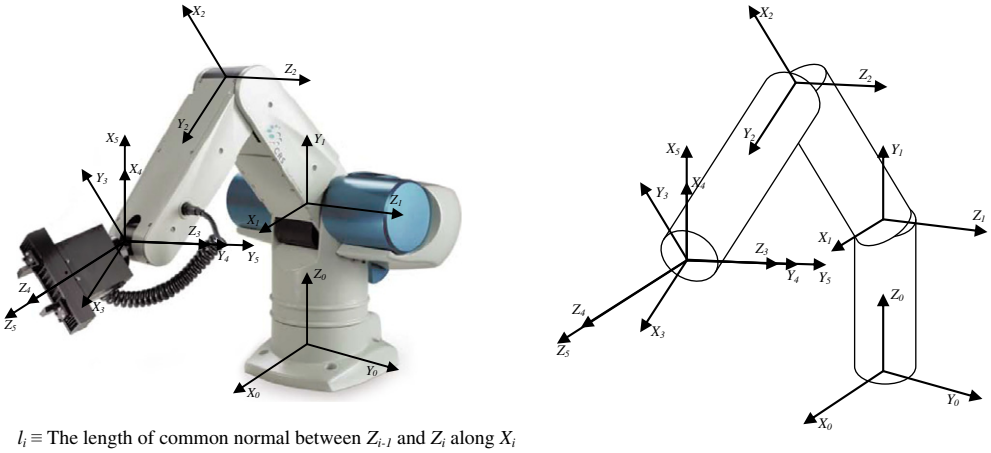

$l_i \equiv$ The length of common normal between Z_{i-1} and Z_i along X_i
$\alpha_i \equiv$ The angel between Z_{i-1} and Z_i measured about X_i
$d_i \equiv$ The distance from X_{i-1} to X_i measured along Z_{i-1}
$\theta_i \equiv$ The angel between X_{i-1} and X_i measured about Z_{i-1}

Fig. 4. The CRS CataLyst-5 manipulator, its schematic and link coordinate frames and D–H parameters.

top) of a vertical (horizontal) power bond is *flow*. This model does not take into account the uncertainty of the design parameters. The generalized executive subsystem consists of the electric motors and the mechanical bodies connected at the joints. The sensory subsystem contains a number of *flow* sensors mounted at the joints, and the control subsystem is composed of n position controllers represented by block diagrams.

The bond graph model of the mechanical subsystem of the robot manipulator is derived based on the exchange of power and movement between the constituents of the physical system, which results in an alternative representation of system dynamics to the Newton–Euler formulation for a generic serial-link manipulator expressed in (30a-c) and (31a,b). The boundary conditions are zero angular and linear velocities (*flow*) at the base and constant force and zero moment (*effort*) at the end-effector. These equations can be extracted by converting the bond graph model of the system to the block diagrams and tracking the appropriate signals in the model [15].

$$ {}^{i}\omega_i = {}^{i}R_{i-1}({}^{i-1}\omega_{i-1} + {}^{i-1}z_{i-1}\dot{\theta}_i); \tag{30a} $$

$$ {}^{i}v_{C_i} = {}^{i}R_{i-1}\,{}^{i-1}v_{i-1} - ({}^{i}\tilde{r}_i + {}^{i}\tilde{r}_{C_i})\,{}^{i}\omega_i; \tag{30b} $$

$$ {}^{i}v_i = {}^{i}R_{i-1}\,{}^{i-1}v_{i-1} - {}^{i}\tilde{r}_i\,{}^{i}\omega_i; \tag{30c} $$

where ${}^{i}\omega_i$ is the angular velocity of link i expressed in frame i, and ${}^{i}v_{C_i}$ and ${}^{i}v_i$ are the linear velocities of the centre of mass and frame origin of link i expressed in frame i, respectively. ${}^{i}R_{i-1}$ is the rotation matrix between frames i and $i-1$, ${}^{i-1}z_{i-1}\dot{\theta}_i$ is the angle between link $i-1$ and i about the joint axis (joint angle), ${}^{i}r_i$ is the distance between the origins of frames i and $i-1$, ${}^{i}r_{C_i}$ is the position of centre of mass of link i, both measured and expressed in frame i. This set of equations shows the *flow* propagation throughout the mechanical subsystem. And,

$$ {}^{i-1}_{i-1}f_{i,i-1} = {}^{i}R^{T}_{i-1}\left({}^{i}_{i}f_{i+1,i} - m^{i}_{i}g + \frac{d}{dt}(m^{i}_{i}v_{C_i})\right); \tag{31a} $$

$$ {}^{i-1}_{i-1}T_{i,i-1} = {}^{i}R^{T}_{i-1}\left({}^{i}_{i}T_{i+1,i} - {}^{i}\tilde{r}_{C_i}\,{}^{i}_{i}f_{i+1,i} + \frac{d}{dt}\left({}^{i}I^{i}_{C_i}\omega_i\right) + ({}^{i}\tilde{r}_i + {}^{i}\tilde{r}_{C_i})\,{}^{i}_{i-1}f_{i,i-1}\right); \tag{31b} $$

where ${}^{i-1}_{i-1}f_{i,i-1}$ and ${}^{i-1}_{i-1}T_{i,i-1}$ are the force and moment acting from link i on link $(i-1)$ at the origin of frame $(i-1)$ and expressed in frame $(i-1)$, m_i is the mass of link i, and ${}^{i}I_{C_i}$ is the moment of inertia of link i about its centre of mass and ${}^{i}g$ is the gravitational acceleration, both expressed in frame i. The skew-symmetric matrices ${}^{i}\tilde{r}_i$ and ${}^{i}\tilde{r}_{C_i}$ are built from ${}^{i}r_i$ and ${}^{i}r_{C_i}$ such that

$$ x = \begin{bmatrix} x_1 \\ x_2 \\ x_3 \end{bmatrix} \Rightarrow \tilde{x} = \begin{bmatrix} 0 & -x_3 & x_2 \\ x_3 & 0 & -x_1 \\ -x_2 & x_1 & 0 \end{bmatrix}. $$

Eqs. (31a) and (31b) reflect flow of *effort* in the bond graph model of the serial-link manipulator.

The bond graph representation of the electric motors consists of two physical domains, i.e., electrical and mechanical. A gyrator element, using the torque coefficient of the motor (K_{m_i}) as the gyrator ratio, relates these two domains. The electrical part includes a voltage supply, a motor driver that is modeled by an amplification gain, and a simple *RL* circuit. Using Kirchhoff's circuit law, for each joint i one can write

$$ \frac{dc_i}{dt} = \frac{1}{l_{m_i}}(u_{a_i} - r_{m_i}c_i - K_{m_i}\dot{\theta}_{m_i}); \tag{32} $$

where c_i, u_{a_i}, θ_{m_i}, l_{m_i} and r_{m_i} are the motor armature current, voltage output of the motor driver, angular displacement of the motor shaft, armature inductance, and total resistance of the armature winding, respectively.

The mechanical domain consists of the motor shaft moment of inertia j_{m_i}, viscous friction at the bearings, and transmission system with ratio η_i. Therefore, the dynamic equation becomes:

$$ \frac{d\dot{\theta}_i}{dt} = \frac{\eta_i}{j_{m_i}}\left(K_{m_i}c_i - \eta_i\tau_i - \frac{\mu_i\dot{\theta}_i}{\eta_i}\right); \tag{33} $$

where θ_i, μ_i and τ_i are the angular displacement of the joint, friction coefficient, and the reaction torque on the ith joint module, respectively. The actuators parameters of the CRS CataLyst-5 have been used in this simulation, as listed in Table 2.

The bond graph model of the robot manipulator was programmed in MATLAB® Simulink and a gradient-based, constrained non-linear optimization algorithm, called *fmincon,* was employed to optimize the design criteria, separately. In each optimization loop, the design variables are changed in the simulation and a design criterion is determined by calculating the power transmission at the corresponding constituents of the system. The cost energy is evaluated based on (20a-c) by calculating $\dot{E}_{in,i}(t)$ at all *effort* sources

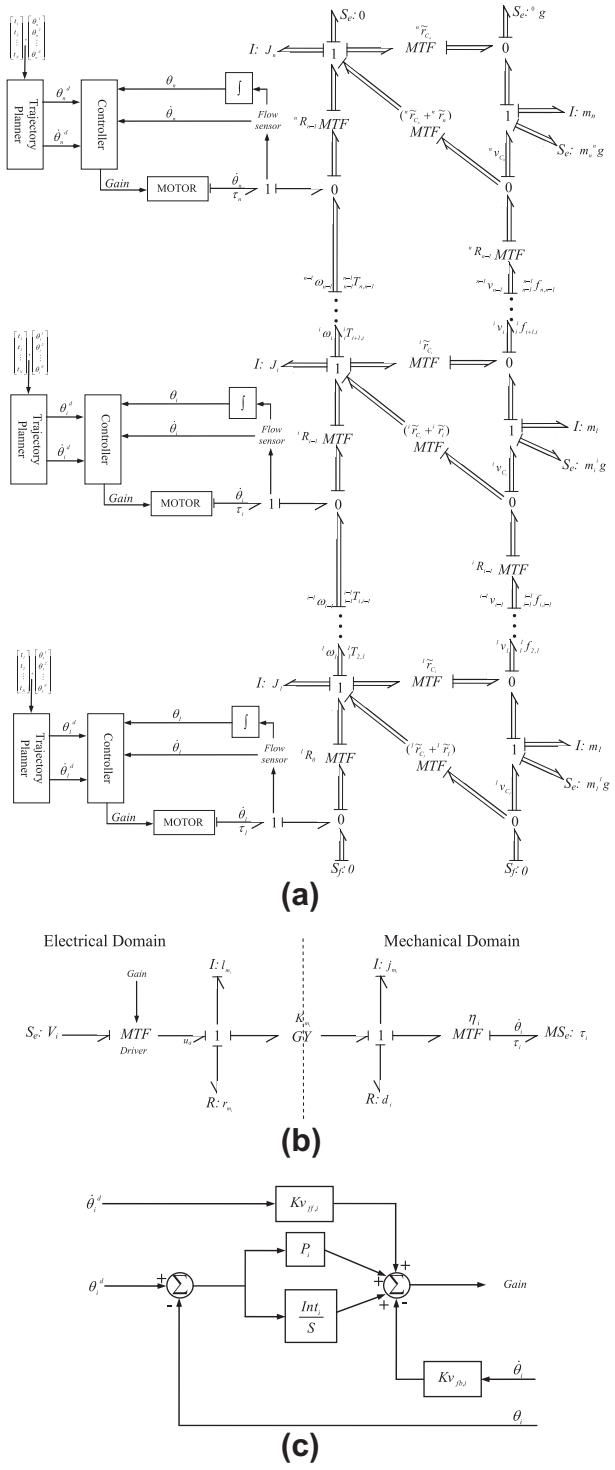

Fig. 5. Bond graph representation of (a) a serial-link manipulator, (b) an electric motor, and (c) the controller block diagram.

in the electric motors and $\dot{W}(t)$ at the *effort* sink in the *EE*. Entropy criterion is calculated by (24) where $\dot{Q}_{irr}$ is equal to the sum of the power transmission at all *R* elements in Fig. 5 and $t_{eq} = t_f$ for all configurations. In the case of agility criterion, all desired angles for joint controllers are given a unit step at $t = 0$. Based on (25a,b) and (26), $i\dot{d}E(t)$ and accordingly *T* are computed by determining power transmission at all *I* elements of the system. The three separate designs based on energy, entropy and agility criterion are shown in Table 3. The initial kinematic, dynamic and control design variables were according to the existing configuration of the CRS CataLyst-5 that was designed through the traditional partitioned approach. In this case study, the intention is to minimize each of the holistic design criteria separately and maintain E_{tot}, defined in (29), below a threshold of 10 mm. It is worth mentioning that having a threshold for E_{tot} results in upper bounds for the final position error and the maximal error of each considered trajectory. These two errors are equally significant in the design of a robot manipulator. In addition, *fmincon* attempts to minimize the constraint, as well as the design criterion. Thus, convergence of the optimization algorithm leads to the convergence of the final position error and the maximal error of each trajectory.

According to Table 3, the design based on the energy criterion results in the reduction of the radius of the first and second links by 16.8% and 6.8%, respectively, and increase of that of the last three links by 31.5%, 122% and 195%, respectively, with respect to the initial configuration. Regarding the kinematic design variables, the length of links 1–5 has changed by +95, −9.1, +3.3, +121.7, +45.6 mm, respectively. Furthermore, the offset for links 1–5 has changed by −65.4 mm, +32.7 mm, +18.4 mm, +37.3 mm and +78.6 mm, respectively. The only significant change in the link twist has happened for link 4 by 36.2%. These modifications result in the change of the mass of first three links for −22.6%, −5.4%,+87.8%, respectively, and the last two links have become 3.9 and 17.5 times heavier, respectively. As a result, the total mass of the robot has been decreased by 1%, which is one reason for reducing the energy consumption at the joints. From the control point of view, the proportional gain of links 2 and 4 has increased by 10% and 13%, respectively. The integral gain of the first, second and fifth links has also increased by 17%, 48% and 62%, respectively. Moreover, the velocity feedback gain of joint 2, 3 and 5 has changed by 14.8%, 18.2% and 25%, respectively. All other control gains have been modified slightly by less than 10% to improve the performance and accuracy of the manipulator. All of the above mentioned changes are in the direction of reducing the overall mass of the robot and increasing the precision and smoothness of the system behaviour to minimize the cost energy. This energy-based design leads to 20.1% reduction in the cost energy, but entropy and agility criteria increase in this design by 7% and 35.9%, respectively.

For the design based on the entropy criterion, the radius of the first three links has changed by +5.5%, −6.5% and −8.3%, respectively. The length of links 1, 4 and 5 has increased by 39.8, 21.1 23.2 mm, respectively, and that of the second and third links has reduced by 26.7 mm. In addition, the twist of links 1, 2 and 4 has changed by 18.9, 8.1 and 8.3 degrees, respectively. These modifications lead to +26.3%, −21.3%, −24.8%, +7.4% and +67.5% change of

Table 2
Motor parameters used in the simulation (CRS CataLyst-5).

	V_i (V)	r_{m_i} (Ohm)	l_{m_i} (mH)	K_{m_i} (N.m/A)	j_{m_i} (g.cm^2)	η_i	μ_i (N.m.s/rad)
Link 1	4	3.3	3	0.2587	68	1/72	0.0001
Link 2	3.6	1.8	2.5	0.4414	300	1/72	0.0001
Link 3	3.6	1.8	2.5	0.4414	300	1/72	0.0001
Link 4	4	3.3	3	0.2587	68	1/19.6	0.0001
Link 5	4	3.3	3	0.2587	68	1/9.8	0.0001

Table 3
Design results.

	$r_i\,(mm)$					$l_i\,(mm)$					$d_i\,(mm)$				
Joint	1	2	3	4	5	1	2	3	4	5	1	2	3	4	5
Initial	65.6	27.7	24.1	10.0	10.0	0.0	254.0	254.0	0.0	0.0	254.0	0.0	0.0	0.0	0.0
Final (Energy)	54.6	25.8	31.7	22.2	29.5	95.0	244.9	257.3	121.7	45.6	188.6	32.7	18.4	37.3	78.6
Final (Entropy)	69.2	25.9	22.1	9.7	10.3	39.8	227.3	227.3	21.1	23.2	248.2	2.2	0.0	0.0	18.7
Final (Agility)	62.3	35.9	27.5	10.7	16.5	57.6	228.3	223.4	16.7	29.0	249.5	57.4	74.9	23.4	33.5
	$\alpha_i(^\circ)$					P_i					Int_i				
Joint	1	2	3	4	5	1	2	3	4	5	1	2	3	4	5
Initial	−90.0	0.0	0.0	−90.0	0.0	20.48	22.26	13.00	12.00	10.05	0.100	0.100	0.150	0.200	0.100
Final (Energy)	−88.6	2.6	7.77	−57.4	17.3	20.17	24.51	12.73	13.58	9.53	0.117	0.148	0.156	0.212	0.162
Final (Entropy)	−71.1	8.3	−1.5	−81.9	−0.2	20.79	23.92	13.34	13.89	12.01	0.095	0.095	0.139	0.184	0.098
Final (Agility)	−83.7	−5.9	13.9	−77.0	0.3	20.14	21.53	14.74	14.56	10.78	0.103	0.101	0.140	0.173	0.093
	$Kv_{fb,i}$					$Kv_{ff,i}$					Criterion			*EE* overall error	
Joint	1	2	3	4	5	1	2	3	4	5	$cE(J)$	$Q_{irr}(J)$	$T(s)$	$E_{tot}(mm)$	
Initial	41.1	39.7	24.1	23.6	22.4	44.38	48.25	33.29	25.00	23.00	21.95	6.39	4.34	18.3	
Final (Energy)	39.3	45.6	28.5	22.1	28.0	44.08	50.38	32.19	26.62	25.01	17.53	6.84	5.90	4.5	
Final (Entropy)	41.7	40.4	25.2	24.6	23.4	46.50	45.00	31.00	28.00	27.00	19.32	4.90	0.55	8.0	
Final (Agility)	40.6	41.5	27.7	24.2	26.4	45.30	45.02	36.00	26.27	24.25	22.23	5.64	0.41	9.2	

the mass of the 5 links, respectively. Considering the control parameters, a notable increase in the proportional gain of the last two links can be observed for 15.7% and 19.5%, respectively. The integral gain of the third and forth links has decreased by 7.3% and 8%, respectively. The feedforward gain of the last four joints has also changed by −6.7%, −6.9%, +12% and +17.4%, respectively. All other design parameters have been modified by less than 5% in order to minimize the design criterion and keep E_{tot} below the threshold. In this design, the irreversible heat exchange has been reduced by 23.3%, and energy and agility criteria have also been enhanced with respect to the initial configuration by 12% and 87%, respectively.

Considering the design solution based on the agility criterion, except for the first link whose radius has decreased by 5%, the radius of the other four links has increased by 29.6%, 14.1%, 7% and 65%, respectively. The length of links 1–5 has changed by 57.6 mm, −25.7 mm, −30.6 mm, 16.7 mm and 29 mm, respectively. Table 3 also shows an increase in the offset of the last four links by 57.4, 74.9, 23.4 and 33.5 mm, respectively. Furthermore, the twist of the first four links has been modified by 6.3, −5.9, 13.9 and 13 degrees, respectively. Overall, these modifications result in +9.3%, +88.1%, +52.8% and +17.3% change in the mass of the first four links, respectively, and the last link has become 3.6 times heavier. Regarding to the control design, the proportional gain of the last three links has increased by 13.4%, 21.3% and 7.3%, respectively. The feedback gain of the third and fifth link has also increased by 14.9% and 17.8%, respectively. Besides, the integral gain of the last three links has decreased by 6.7%, 13.5% and 7%, respectively. In terms of the feedforward gain, links 2 and 3 show a change of −6.7% and +8.1%, respectively. The rest of the design parameters have been modified by maximum 5%. As a result, for step input trajectories the manipulator response is almost 10 times faster and the energy and entropy criteria have changed by +1.3% and −11.7%, respectively.

Fig. 6 depicts the average of the *EE* position error, formulated in (28), for a set of desired trajectories considered in the design, including step, ramp, pick-and-place, and periodic. For all of the design solutions the error variation for almost the entire operation time remains below the error curve for the initial configuration. The *EE* overall error, E_{tot}, for the initial and alternative designs is calculated from (29) and listed in Table 3. For the design based on energy, entropy and agility criteria E_{tot} has decreased by 75%, 56.4% and 49.5%, respectively. Note that the end-effector error for the initial configuration is 18.0 mm, which is more than the

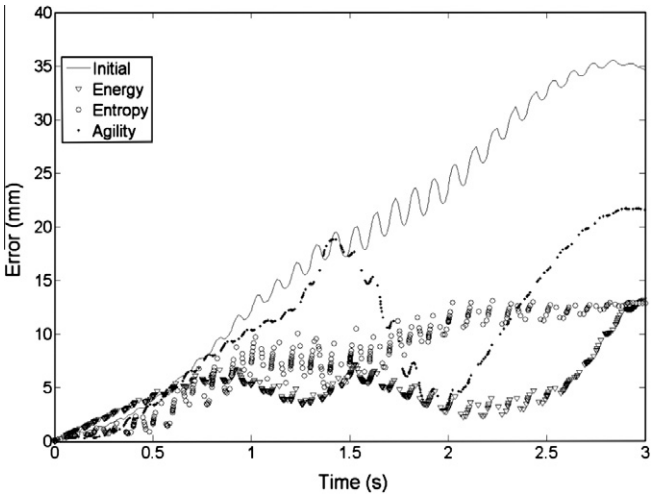

Fig. 6. The average of end-effector position error for a set of desired trajectories based on different criteria.

10 mm threshold set in the design. An interesting observation is the way that each design criterion affects the error variation. The agility criterion seems to result in relatively high error variations, due to the fact that it attempts to speed-up the system response, while by finding a proper combination of control gains and kinematic and dynamic parameters it tries to maintain the overall error below the threshold. In case of energy criterion, the system response begins by a slightly larger error but tends to rather smooth out the error variation, because energy criterion does not favour drastic control commands at the joints to save energy. The entropy criterion attempts to reduce the wasted irreversible energy, in the form of heat generated by friction and electric resistance. This is reflected in the end-effector error response as a relatively constant curve with local oscillations to ensure that the equilibrium time remains as short as possible.

From Table 3, all three design solutions result in notable changes in kinematic, dynamic, and control parameters compared to those of the existing design of the CRS CataLyst-5 manipulator. Each solution improves the corresponding criterion as well as the *EE* overall error. Nonetheless, the entropy-based design seems to enhance all three design criteria simultaneously, and hence it could present a reasonable compromise for all three criteria and the *EE* overall error.

7. Conclusions

In this paper, mechatronic systems were deemed as energy systems, and first and second laws of thermodynamics were reformulated for defining several design criteria using bond graph notation. This holistic system modeling approach is suitable for concurrent design of mechatronic systems. Three design criteria, namely energy, entropy and agility, were introduced. The choice of the criterion for a design problem is up to the designer, and it also depends on the critical performance measures. For instance, for designing many systems that are used in the space industry where power efficiency is important, energy criterion can be employed, whereas for thermodynamic systems entropy criterion is usually appropriate, and for systems that are designed to operate fast, agility criterion can be optimized. As a case study, the bond graph model of a five d.o.f. industrial serial-link manipulator was developed, and its kinematic, dynamic, and control parameters were re-designed concurrently through optimizing each of the developed holistic design criteria separately. The resulting designs show superior performance compared to the existing manipulator configuration, which highlights the significance of synergy in the design of mechatronic systems through proper means.

References

[1] Habib MK. Mechatronics. IEEE Ind Electr Mag 2007;1(2):12–24.
[2] Roe P. Networks and systems. 1st ed. Reading, MA: Addison-Wesley; 1966.
[3] Lang SYT, Kesavan HK. Graph theoretic modeling and analysis of multibody planar mechanical systems. IEEE Trans Syst Man Cybern 2001;31(2):97–111.
[4] Scherrer M, McPhee J. Dynamic modeling of electromechanical multibody systems. Multibody Syst Dyn 2003;9:87–115.
[5] McPhee J, Schmitke C, Redmond S. Dynamic modeling of mechatronic multibody systems with symbolic computing and linear graph theory. Mech Comput Model Dyn Syst 2004;10(1):1–23.
[6] McPhee J. On the use of linear graph theory in multibody system dynamics. Nonlinear Dyn 1996;9:73–90.
[7] Paynter HM. Analysis and design of engineering systems. Cambridge, MA, USA: MIT Press; 1961.
[8] Breedveld PC. Port-based modeling of mechatronic systems. Mech Comput Simul 2004;66:99–127.
[9] Borutzky W. Bond graph modeling and simulation of mechatronic systems: an introduction into the methodology. In: Proceedings 20th European conference on modeling and simulation; 2006.
[10] Tiernego MJL, Bos AM. Modeling the dynamics and kinematics of mechanical systems with multibond graphs. J Franklin Inst 1985;319(1/2):37–50.
[11] Jang J, Han C. Proposition of a modeling method for constrained mechanical systems based on the vector bond graph. J Franklin Inst 1998;335B(3):451–69.
[12] Gawthrop PJ. Bond graphs: a representation for mechatronic systems. Mechatronics 1991;1(2):127–56.
[13] Fotsu-Ngwompo R, Scavarda S, Thomasset D. Bond graph methodology for the design of an actuating system: application to a two-link manipulator. Proc IEEE Int Conf Syst Man Cybern 1997;3:2478–83.
[14] Amerongen JV. Mechatronic design. Mechatronics 2003;13:1045–66.
[15] Karnopp DC, Margolis DL, Rosenberg RC. System dynamics modeling and simulation of mechatronic systems. 4th ed. New Jersey: John Wiley and Sons; 2006.
[16] Seo K, Fan Z, Hu J, Goodman ED, Rosenberg RC. Toward a unified and automated design methodology for multi-domain dynamic systems using bond graphs and genetic programming. Mechatronics 2003;13:851–85.
[17] Affi Z, EL-Kribi B, Romdhane L. Advanced mechatronic design using a multi-objective genetic algorithm optimization of a motor-driven four-bar system. Mechatronics 2007;17:489–500.
[18] Rui-qin L, Hui-jun Z. A new symbolic representation method to support conceptual design of mechatronic system. Int J Adv Manuf Technol 2005;25:619–27.
[19] Denavit J, Hartenberg RS. A kinematic notation for lower-pair mechanisms based on matrices. J Appl Mech 1955;77:215–21.